

Assessment of the Statistical Impedance Field Method for the Analysis of the RTN Amplitude in Nanoscale MOS Devices

Giulio Torrente*, Niccolò Castellani*, Andrea Ghetti[†], Christian Monzio Compagnoni*,
Andrea L. Lacaita*[‡], Alessandro S. Spinelli*[‡], Augusto Benvenuti[†]

* Dipartimento di Elettronica, Informazione e Bioingegneria, Politecnico di Milano, piazza L. da Vinci 32, 20133 Milano, Italy

[†] Micron Technology Inc., Process R&D, 20864 Agrate Brianza (MB), Italy

[‡] IFN-CNR, Milano, Italy

Abstract—This work investigates the performance of the statistical impedance field method in the analysis of the amplitude of random telegraph noise fluctuations in nanoscale MOS devices. Considering different channel doping profiles, we show that this method offers a practical compromise between accuracy and computational loads, allowing a good assessment of the RTN amplitude statistics while resulting in non-negligible errors on the single microscopic samples where atomistic doping strongly contributes to non-uniformities of channel inversion and to percolative source-to-drain conduction.

Keywords: MOSFETs, Flash memories, random telegraph noise, statistical impedance field method, semiconductor device modeling.

I. INTRODUCTION

Random Telegraph Noise (RTN) represents one of the most challenging reliability issues for nanoscale MOS devices and the statistical analysis of its features is a mandatory task to fully understand its impact on state-of-the-art technologies. In particular, the statistical distribution of the RTN amplitude is an extremely important piece of information for digital components, such as SRAM and Flash memories, where the large number of devices per chip requires the exploration of the distribution down to very low probability levels [1]–[3]. From the numerical simulation standpoint, this can be hardly achieved by conventional Monte Carlo (MC) approaches reproducing in the simulation domain microscopic differences in device structure, pushing for the search of new numerical schemes with less demanding computational burdens.

In this work, we show that the statistical Impedance Field Method (sIFM) [4] offers a practical compromise between accuracy and computational loads in the analysis of the RTN amplitude of nanoscale MOS devices. Considering various channel doping profiles and following an MC approach to gather statistical results on samples with different atomistic doping configurations, which are not numerically implemented in the simulator but dealt with in a simplified manner, we show that the sIFM allows a good assessment of the RTN amplitude statistics, despite failing in correctly addressing the single MC samples where atomistic doping largely compromises the uniformity of channel inversion. The loss in accuracy, however, is compensated by a strong reduction of the computational

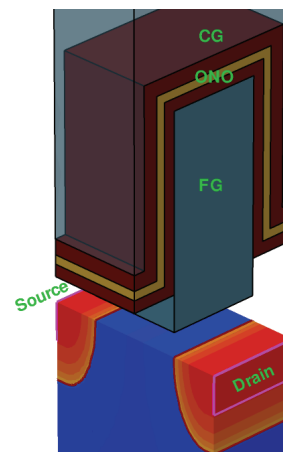


Fig. 1. Schematics for the Flash cell investigated in this work.

requirements of the method, allowing, in turn, the exploration of the RTN statistics down to lower probabilities than those accessible by conventional MC approaches.

II. NUMERICAL APPROACH

We investigated the amplitude of RTN fluctuations on the template Flash cell shown in Fig. 1, representing just a test case for our analysis. The device features an 8 nm tunnel oxide, a 70 nm polysilicon floating gate, a 4-3-5 nm oxide-nitride-oxide (ONO) interpoly dielectric and a uniform substrate doping $N_A = 2 \times 10^{18} \text{ cm}^{-3}$ (except were noted). Cell width and length are $W = L = 32 \text{ nm}$. The RTN amplitude statistics was calculated according to two different MC approaches, both giving the drain current vs. control-gate voltage (I_D - V_{CG}) characteristics (drain bias $V_D = 100 \text{ mV}$) of a large number of samples having a different atomistic doping configuration and a single (randomly placed) RTN trap at the channel surface. The first method (used as reference) is the conventional MC scheme consisting in the Poisson/drift-diffusion simulation of each sample reproducing in the numerical domain the atomistic nature of doping [5], [6]. The second one, instead, makes use of the sIFM [4] for the calculation of

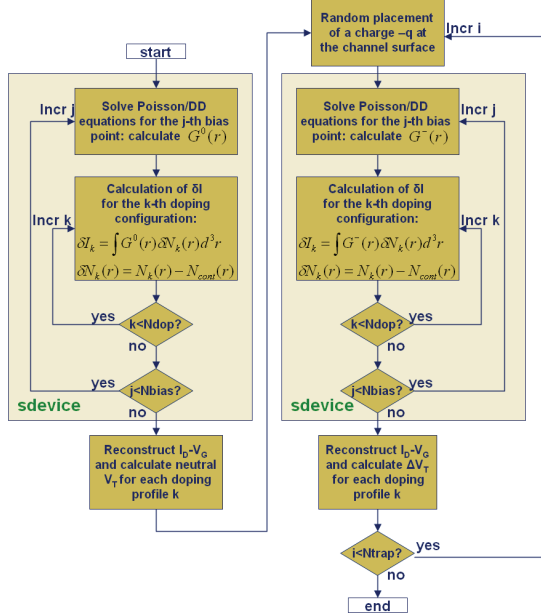


Fig. 2. Block diagram for the sIFM scheme considered in this work. Shaded blocks are directly managed by the commercial simulator SDevice [8].

the I_D - V_{CG} curve as shown in Fig. 2. For each bias point, the Green Function G^0 is first calculated from the solution of the Poisson/drift-diffusion equations in the case of continuous doping and neutral RTN trap. Then, N_{dop} configurations of dopants are generated and, for each of them, the I_D difference (δI_D) from the case of continuous doping is calculated as shown in the figure, namely, considering G^0 as the impulsive response to a local variation of doping with respect to the continuous case [4], [7]. Repeating this procedure for each V_{CG} , the I_D - V_{CG} curve is calculated for each doping configuration, giving the corresponding neutral threshold voltage (V_T) as the V_{CG} value required for the condition $I_D = 100$ nA to hold. In order to deal with the negatively charged RTN trap case, then, a new Green function (G^-) is calculated from the Poisson/drift-diffusion solution obtained in the case of continuous doping when a single elementary charge $-q$ is added at the channel surface. Using G^- , new I_D - V_{CG} curves are calculated for the previously investigated ensemble of atomistic doping configurations, obtaining, for each of them, the amplitude ΔV_T of the fluctuation given by the RTN trap placed at the position of the charge $-q$ as the V_T shift with respect to the neutral V_T . In order to explore different trap positions, the calculation of the I_D - V_{CG} curve in presence of the filled RTN trap was repeated N_{trap} times, thus obtaining a total number of $N_{trap} \times N_{dop}$ ΔV_T values.

III. RESULTS

Fig. 3 shows the sIFM-simulated I_D - V_{CG} curve of some atomistic doping configurations of the device of Fig. 1, in the case of neutral RTN trap. In order to quantitatively compare these results with those obtained from the reference MC method, the cumulative distribution of neutral cell V_T is

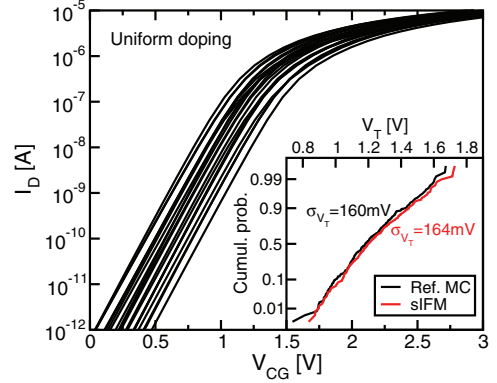


Fig. 3. I_D - V_{CG} curves for some of the atomistic doping configurations of the device of Fig. 1, as resulting from the sIFM in the case of empty RTN trap. Inset shows the V_T (@100 nA) cumulative distribution from the sIFM and the reference MC method.

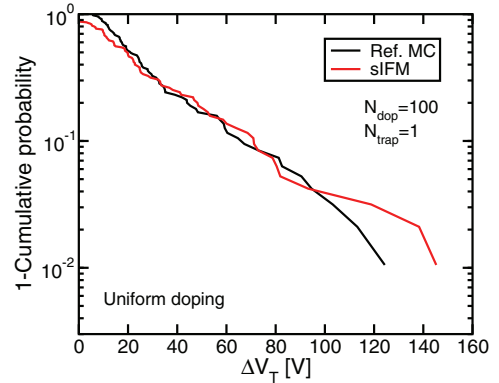


Fig. 4. ΔV_T cumulative distribution as resulting from the reference MC method and the sIFM.

reported in the inset: a good agreement between the distributions resulting from the two methods appears in terms of both average value and standard deviation, confirming the validity of the sIFM for the investigation of atomistic doping effects on neutral V_T [4]. Fig. 4 shows, moreover, that the sIFM can also correctly reproduce the statistical distribution of the RTN amplitude ΔV_T coming from the reference MC method, following an exponential trend with average value $\langle \Delta V_T \rangle \simeq 31$ mV [6] (note that both the sIFM and the reference MC simulations were performed on the same set of microscopic cells, with $N_{dop} = 100$ and $N_{trap} = 1$).

Notwithstanding the good matching of the ΔV_T statistics, Fig. 5 reveals non-negligible displacements between the sIFM and the reference MC results when directly considering the ΔV_T of the single microscopic samples. In particular, errors in the sIFM scheme may consist either in an underestimation or in an overestimation of the real ΔV_T of the samples with similar probability (see the similar dispersion of the points of the scatter plot about the graph bisector), explaining why these inaccuracies do not critically impact the statistical results of Fig. 4. These errors are the direct consequence of the linear approximations involved in the solution of the

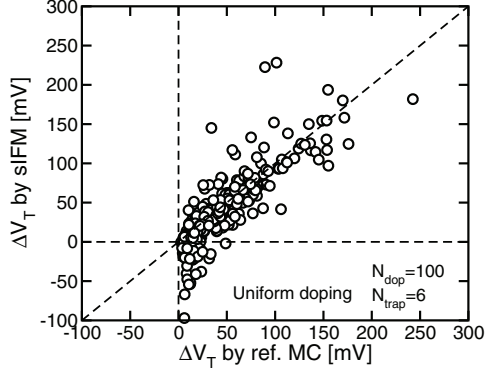


Fig. 5. Scatter plot for the sIFM and reference MC ΔV_T .

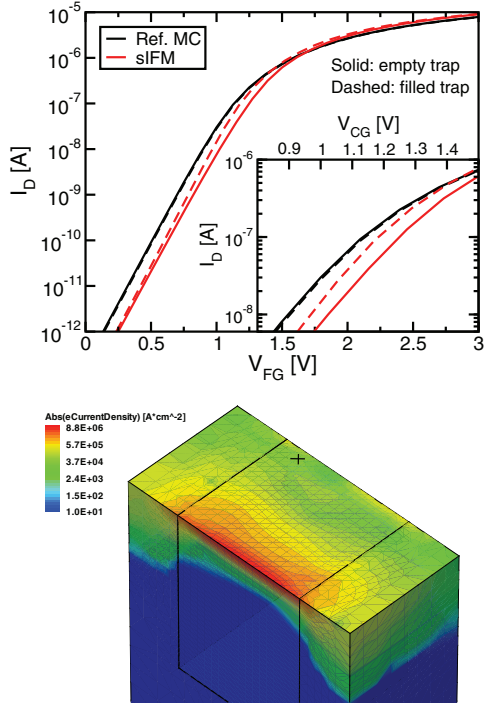


Fig. 6. Top: Simulated I_D - V_{CG} curve for a cell leading to the unphysical results of a negative ΔV_T after electron trapping in sIFM calculations. Results from the reference MC method are also shown. Bottom: Corresponding electron current density at threshold in the case of empty RTN trap, whose position is highlighted with a \times .

Poisson/drift-diffusion equations in the sIFM [4], [7], making critical dealing with doping configurations leading to highly non-uniform channel inversion and strong percolative source-to-drain conduction. Fig. 5 shows that the resulting errors in the sIFM may be so large to predict the unphysical result of a negative ΔV_T after electron trapping in some cases. One of these cases is addressed in Fig. 6, showing that the sIFM largely fails in determining the cell I_D - V_{CG} curve both for the empty and for the filled trap state. The strong impact of atomistic doping on cell conduction in this case clearly appears in the current density profile at threshold, highlighting a strong percolation path along one of the active area edges and the presence of the RTN trap over the other one.

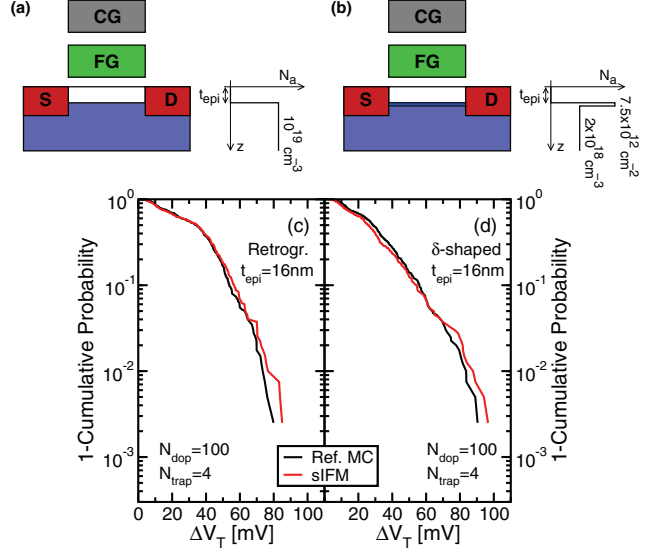


Fig. 7. Schematics for the cell structure considered in this work to investigate a vertically non-uniform doping profile and corresponding ΔV_T cumulative distribution, as resulting from the sIFM and the reference MC method. (a) and (c) refer to a retrograde channel doping, (b) and (d) to a δ -shaped profile. The thickness of the undoped epitaxial layer is in both cases $t_{epi} = 16$ nm.

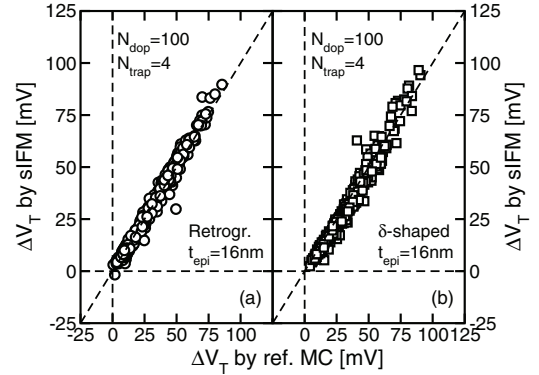


Fig. 8. Same as in Fig. 5, but for the doping profiles of Fig. 7a-b.

Fig. 7 extends our analysis of the sIFM to devices with a vertically non-uniform channel doping, consisting in a retrograde (Fig. 7a-c) or in a δ -shaped (Fig. 7b-d) profile with a thickness of the undoped epitaxial layer $t_{epi} = 16$ nm. These profiles aim at reaching a more uniform channel inversion by keeping ionized dopants far from the silicon surface, thus reducing neutral V_T variability [9] and narrowing the RTN amplitude statistics [10]. In both the doping cases, the sIFM appears to correctly reproduce the ΔV_T statistics coming from the reference MC scheme, further validating the method when looking at the ensemble of the ΔV_T values. Moreover, Fig. 8 reveals that, in contrast with what shown for uniform doping in Fig. 5, the sIFM in these cases correctly deals also with each individual MC sample, nicely matching each single ΔV_T coming from the reference MC method. This is the result of a lower impact of atomistic doping on channel inversion when dopants are far from the silicon surface, making the linear

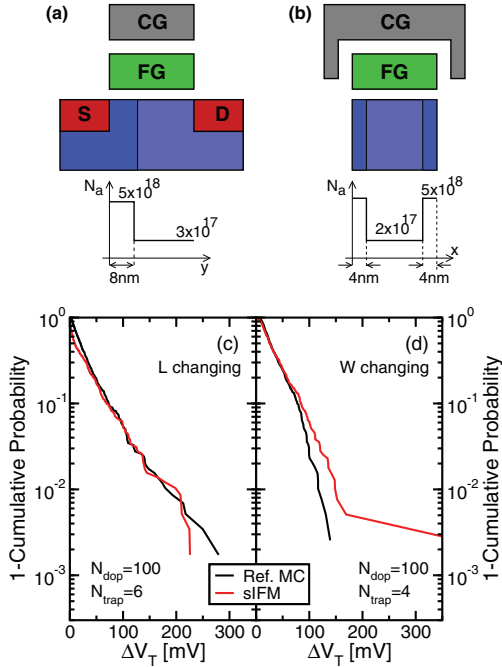


Fig. 9. Same as in Fig. 7 but for a doping profile changing along L (see (a) and (c)) and along W (see (b) and (d)). Doping concentrations are in cm^{-3} .

approximations involved in the sIFM more valid. To complete our analysis, Fig. 9 shows that the sIFM succeeds also in reproducing the ΔV_T statistics of the reference MC method when considering a non-uniform doping profile changing along L (Fig. 9a-c), while being less accurate when dealing with a doping change in the W direction (Fig. 9b-d).

The agreement between the sIFM and the reference MC results on the ΔV_T statistics allows to exploit the key benefit of the sIFM, *i.e.*, its reduced computational loads. Note, in fact, that the sIFM requires the correct solution of the Poisson/drift-diffusion equations only in the case of continuous doping, for the neutral and the filled trap states. As the solution for the neutral state of all the N_{trap} cases coincides, this means that these equations are to be solved $N_{trap} + 1$ times to gather a statistics of $N_{trap} \times N_{dop}$ values of ΔV_T , with a significant reduction of the computational burdens. This, in turn, means that for the same computational efforts, the sIFM allows to explore the ΔV_T statistics down to lower probability levels than the reference MC method. This was done, for instance, in Fig. 10, where the statistical distribution of ΔV_T resulting from the sIFM is extended down to $\simeq 10^{-4}$ for all of the explored channel doping profiles. This allows to better appreciate the impact of non-uniform doping on the RTN amplitude distribution, highlighting its strong narrowing when a retrograde or a δ -shaped doping is adopted and the possibility either to enlarge or to narrow the distribution at low probabilities through L -changing or W -changing profiles.

IV. CONCLUSIONS

We showed that the sIFM represents a valid compromise between accuracy and computational loads in the statistical

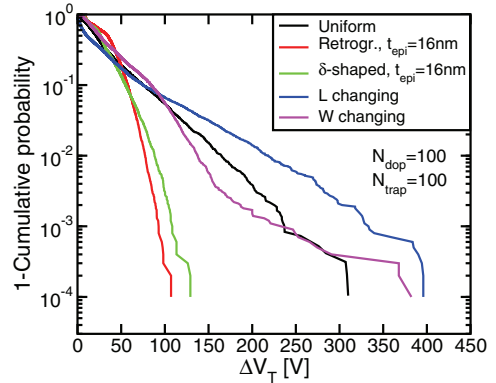


Fig. 10. ΔV_T statistics for all the doping profiles investigated in this work, as resulting from the sIFM in the case of $N_{dop} = 100$ and $N_{trap} = 100$.

analysis of the RTN amplitude of nanoscale MOS devices with different doping profiles, allowing a good assessment of the ΔV_T statistics while committing non-negligible errors on single microscopic samples where uniformity of channel inversion is strongly compromised by atomistic doping.

V. ACKNOWLEDGMENTS

The authors would like to thank A. Mauri, G. Carnevale and A. Marmiroli from Micron Technology Inc. and S. Donati and F. Bonani from Politecnico di Torino for helpful discussions.

REFERENCES

- [1] H. Kurata, K. Otsuga, A. Kotabe, S. Kajiyama, T. Osabe, Y. Sasago, S. Narumi, K. Tokami, S. Kamohara, and O. Tsuchiya, "The impact of random telegraph signals on the scaling of multilevel Flash memories," in *Symp. VLSI Circ. Dig.*, pp. 140–141, 2006.
- [2] R. Gusmeroli, C. Monzio Compagnoni, A. Riva, A. S. Spinelli, A. L. Lacaita, M. Bonanomi, and A. Visconti, "Defects spectroscopy in SiO_2 by statistical random telegraph noise analysis," in *IEDM Tech. Dig.*, pp. 483–486, 2006.
- [3] N. Tega, H. Miki, M. Yamaoka, H. Kume, T. Mine, T. Ishida, Y. Mori, R. Yamada, and K. Torii, "Impact of threshold voltage fluctuation due to random telegraph noise on scaled-down SRAM," in *Proc. IRPS*, pp. 541–546, 2008.
- [4] K. El Sayed, A. Wettstein, S. D. Simeonov, E. Lyumkis, and B. Polsky, "Investigation of the statistical variability of static noise margins of SRAM cells using the statistical impedance field method," *IEEE Trans. Electron Devices*, vol. 59, pp. 1738–1744, June 2012.
- [5] A. Asenov, R. Balasubramaniam, A. R. Brown, and J. H. Davies, "RTS amplitudes in decanometer MOSFETs: 3-D simulation study," *IEEE Trans. Electron Devices*, vol. 50, pp. 839–845, Mar. 2003.
- [6] A. Ghetti, C. Monzio Compagnoni, A. S. Spinelli, and A. Visconti, "Comprehensive analysis of random telegraph noise instability and its scaling in deca-nanometer Flash memories," *IEEE Trans. Electron Devices*, vol. 56, pp. 1746–1752, Aug. 2009.
- [7] A. Wettstein, O. Penzin, E. Lyumkis, and W. Fichtner, "Random dopant fluctuation modelling with the impedance field method," in *SISPAD Conf. Proc.*, pp. 91–94, 2003.
- [8] Synopsys, Zurich, Switzerland, *Sentaurus device user guide*, G-2012.06 ed., 2012.
- [9] A. Asenov and S. Saini, "Suppression of random dopant-induced threshold voltage fluctuations in sub-0.1 μm MOSFET's with epitaxial and δ -doped channels," *IEEE Trans. Electron Devices*, vol. 46, pp. 1718–1724, Aug. 1999.
- [10] A. Ghetti, S. M. Amoroso, A. Mauri, and C. Monzio Compagnoni, "Impact of nonuniform doping on random telegraph noise in Flash memory devices," *IEEE Trans. Electron Devices*, vol. 59, pp. 309–315, Feb. 2012.